MTLA 36 (2024) 102148

Contents lists available at ScienceDirect

Materialia

journal homepage: www.elsevier.com/locate/mtla

Full length article

The origin of phase separation in binary aluminosilicate glasses

Houssam Kharouji [a,b], Abdellatif Hasnaoui [b], Achraf Atila [c,*]

[a] LEM3, Labex Damas, Université de Lorraine, Metz, 57070, France
[b] LS2ME, Faculté Polydisciplinaire Khouribga, Sultan Moulay Slimane University of Beni Mellal, B.P 145, 25000 Khouribga, Morocco
[c] Department of Material Science and Engineering, Saarland University, Saarbrücken, 66123, Germany

ARTICLE INFO

Keywords:
Phase separation
Aluminosilicate glasses
Atomistic simulation
Chemical order
Structure

ABSTRACT

The quest for hard and tough transparent oxide glasses is at the core of glass science and technology. Aluminosilicate glasses exhibiting nanoscale phase separation emerge as promising candidates for such materials. Nevertheless, proper control of the phase separation represents a daunting challenge due to its elusive origins. Here we employ large-scale molecular dynamics simulations and structural analysis to unravel the underlying mechanisms of the phase separation in aluminosilicate. The observed phase separation originates from an arrangement of SiO_4 and AlO_n polyhedra, which manifests from the second coordination shell and extends to higher shells. This specific arrangement is driven by repulsion between the polyhedra, reaching its maximum at around 50 mol% of Al_2O_3. This behavior becomes pronounced around and below the glass transition temperature. This work sheds light on the origin of phase separation and provides a route for further exploration across other compositions to develop glasses with adapted mechanical performance.

Oxide glasses are used in a wide range of applications, enabling modern civilization, e.g., optical fibers [1], bioactive materials [2,3], solar cells [4], and flexible and foldable screens for mobile devices [5]. The usage of oxide glasses in these applications benefits from their excellent optical properties [6,7], chemical durability [8], and the high tailorability of the properties through compositional design [2,9], (post-) processing [10,11], or a combination thereof [12]. However, the brittleness of these glasses, which is due to the lack of a stable shearing mechanism that accommodates the deformation, has limited the development of existing and emerging glass applications [13]. Thus, the need for new glasses with adapted mechanical properties triggered efforts to achieve this goal [14–19].

For instance, the use of reinforcements has been proven effective in controlling crack propagation [20], but it affects the glass transparency [21]. Glasses with nanoscale phase separation were observed to improve fracture toughness compared to homogeneous glasses [22,23]. The mechanism of enhancing the hardness and fracture toughness of glasses with phase separation works in principle in the same way as for a composite material with two interconnected glassy regions with different structures, i.e., a rigid one and the other one is more flexible [18,23,24].

Binary aluminosilicate glasses with nanoscale phase separation are great potential candidates to make glasses with high hardness and crack resistance [19,25]. Rosales-Sosa et al. studied aluminosilicate glasses with alumina content ranging between 30 and 60 mol% and showed that the increase in the elastic moduli, hardness, and cracking resistance of binary aluminosilicate glasses was due to the increase in the atomic packing density, the high dissociation energy per unit volume of Al_2O_3 compared to that of SiO_2, and increase in the glass density with increasing Al_2O_3 content [19]. While the explanations from Ref. [19] are indeed valid, they neglect the presence of a phase separation, which shows a maximum at the compositions with an alumina content around 50 mol% [26–32], and its effects on the observed behavior. Macdowell et al. highlighted that the composition at which the alumina content is around 50 mol% shows the highest degree of phase separation [26]. While others showed that the maximum phase separation occurs around 60 mol% of Al_2O_3 [31,33]. Recently, Urata et al. [34] used molecular dynamics simulations to study the co-doping effect of alumina and fluorine on the density fluctuations in silica glass. In their study, they also observed phase separation in binary aluminosilicate glasses in the simulated samples. Although they reported phase separation, no indication of its origins or deeper insights was given.

Although phase separation has been observed in binary [34–37], ternary [38] aluminosilicate, and other oxide glasses [39], its origins remain elusive. Here we used a million atoms molecular dynamics (MD) simulations to study the phase separation in aluminosilicate glasses with Al_2O_3 content ranging between 10 and 90 mol%. We found that this phase separation is discernible through changes in the medium-range structure, starting from the second coordination shell

* Corresponding author.
E-mail address: achraf.atila@uni-saarland.de (A. Atila).

https://doi.org/10.1016/j.mtla.2024.102148
Received 17 February 2024; Accepted 2 June 2024
Available online 5 June 2024

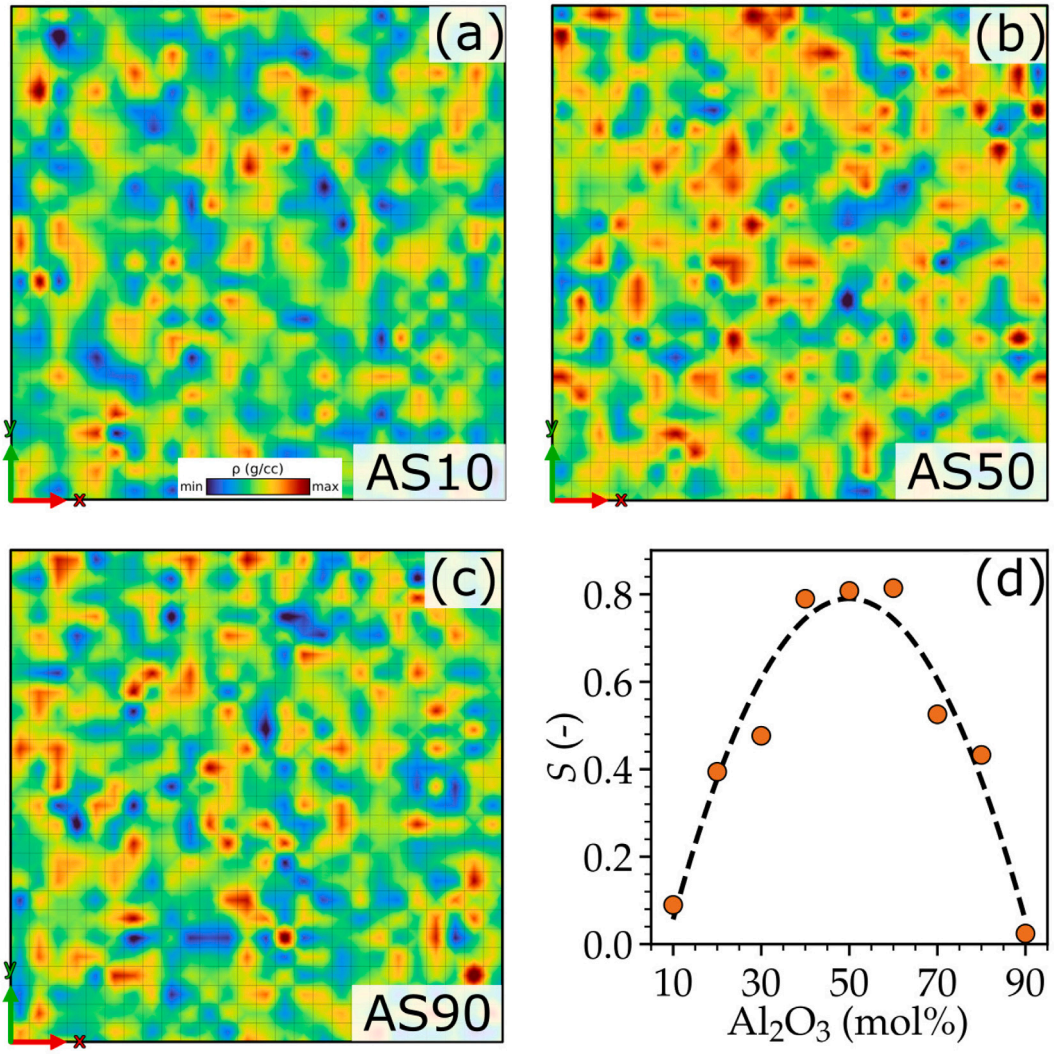

Fig. 1. (a–c) Selected local density maps of binary aluminosilicate glasses. The density maps are for (a) x = 10 mol%, (b) x = 50 mol%, and (c) x = 90 mol%. The simulation boxes were divided to produce small cubes of volume, 10 × 10 × 10 Å^3, and then the density of each cube was calculated and used for further analysis. In (d), the skewness is plotted as a function of the composition at 300 K. The skewness is obtained by fitting the histograms of local density to a skewed Gaussian function (See Supplementary material for details). The dashed line is fit to a quadratic function and serves as a guide to the eye (For interpretation of the colors in the figure(s), the reader is referred to the web version of this article).

and extending to larger shells. Furthermore, our MD results indicate an absence of any significant phase separation in the liquid state at elevated temperatures, and signs of phase separation were observed only in the supercooled liquid around the glass transition temperature (T_g) and below it.

All MD simulations were performed using LAMMPS [40]. The potential from Bouhadja et al. [41,42] was used to model the interactions between atoms. The glass composition of the binary aluminosilicate glasses has Al_2O_3 content ranging between 10 mol% to 90 mol%, with samples named ASx with x is the molar content of Al_2O_3. The glass was equilibrated at 5000 K and cooled using 1 K/ps to room temperature (300 K). Configurations at different temperatures during the cooling process were extracted for further analysis. More details about the glass preparation can be found in Ref. [43] and the supplementary materials (SM). The visualizations are made using OVITO [44]. The structure of the glass is in realistic agreement with the data available in the literature [41,45,46] as discussed in the SM and shown in Fig. S2, Fig. S3, Fig. S4, and Tab. S1.

The phase separation was visually observed in the simulated aluminosilicate glasses with different degrees as illustrated from selected compositions in Fig. 1(a–c) using the 2D spatial distribution of the mass density. The histograms of the density distribution throughout the system are shown in the SM, Fig. S5, which were fitted using a skewed Gaussian distribution function (details in the SM) to extract the skewness S. If the glass is homogeneous, then the density distribution should be well described through a Gaussian function, with its skewness being nearly 0. On the other hand, if the glass has phase separation, the density distribution can no longer be described through a symmetric Gaussian function, and it will be skewed. The higher the values of the skewness, the higher the asymmetry of the distribution. The values of the skewness S are plotted as a function of the alumina content and show a maximum at composition around 50 mol% of Al_2O_3.

The glasses are expected to be more homogeneous at the compositions at which the SiO_2 content is very high or very low. The presence of inverted parabolic-like behavior of S with the alumina content and the occurrence of a maximum at around 50 mol% of Al_2O_3 is consistent with the hypothesis stating that the maximum phase separation is around 50 mol% of Al_2O_3. These results are in good agreement with experiments and theoretical studies, although there is disagreement regarding the value of the critical composition of demixing in binary AS glasses [27,29,47].

From an atomistic point of view, the tendency to phase separate in AS glasses could be correlated with the preference of SiO_4 and AlO_n (with n = 4,5, or 6) polyhedra to be surrounded by those of the same

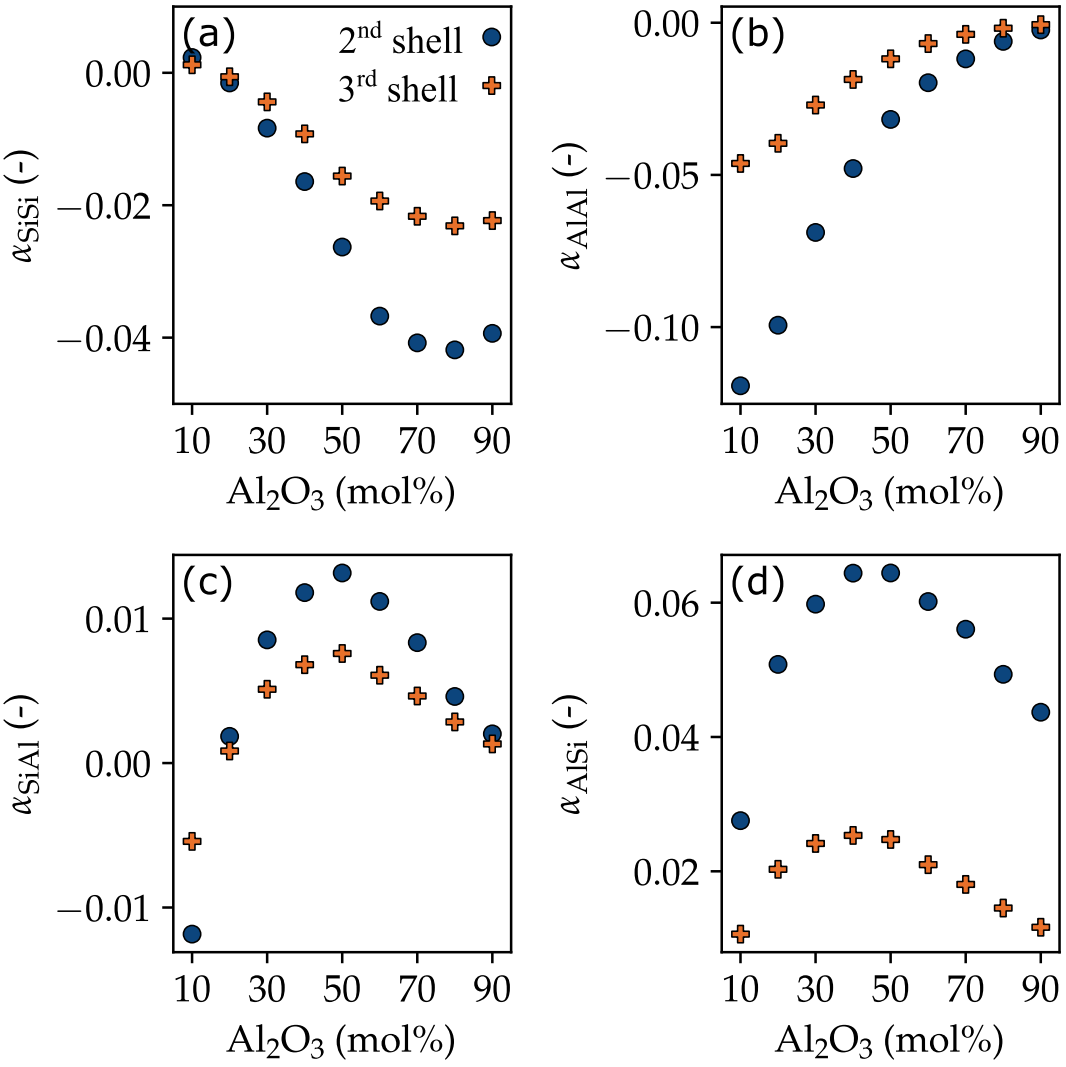

Fig. 2. Chemical short-range order at the second and third shell as a function of the alumina content at 300 K. (a) Si–Si, (b) Al–Al, (c) Al–Si, and (d) Si–Al. The standard error bars are smaller than the symbol size. We note that an exact determination of the higher coordination shells in amorphous materials is far from trivial. Thus, $r_{cut}^{2^{nd}shell} = 5.35$ Å and $r_{cut}^{3^{rd}shell} = 9.1$ Å. The values of the cutoff radii are provided for better reproducibility of the results. (For interpretation of the colors in the figure(s), the reader is referred to the web version of this article).

type. This process is evaluated with the distance-dependent Warren-Cowley (WC) order parameter defined for a pair of atom types i, j as follows [11,48]:

$$\alpha_{ij}(r) = 1 - \frac{n_{ij}(r)}{N_i(r)c_j}, \tag{1}$$

where $n_{ij}(r)$ is the number of atoms of type j neighbors of a central atom of type i at a distance r, $N_i(r)$ is the total of neighbors for the atom of type i at a distance r, c_j is the concentration of type j. Negative values of α_{ij} indicate attraction between the pairs, while positive values correspond to the opposite. Throughout this paper, we limited the calculation of α_{ij} to Si and Al atoms without involving oxygen atoms to extract the correlations between SiO_4 and AlO_n polyhedra with n = 4, 5, or 6. Fig. S6 represents the variation of this order parameter in the first coordination shell, defined by the first minimum of the radial distribution function, as a function of Al_2O_3 content. The calculated α_{SiSi} is slightly higher than zero up to $x = 0.6$, where it starts to increase. At low Al_2O_3 content, α_{SiAl} is negative and increases with increasing Al_2O_3 content. This indicates a preference for Si to have Al in their first neighboring shell, which decreases with increasing alumina. On the other hand, α_{AlSi} is always positive, highlighting that AlO_n polyhedra do not prefer SiO_4 tetrahedra as neighbors and indicating a relatively low probability of having SiO_4 tetrahedra around an AlO_n polyhedra in the first shell. The WC parameter for Al–Al is negative at low alumina content and increases with increasing Al_2O_3. This indicates that there is a strong attraction between AlO_n and AlO_n polyhedra, and AlO_n prefers to have other AlO_n polyhedra in their first neighboring shell, which becomes less pronounced with increasing Al_2O_3.

Since the data obtained from the α_{ij} up to the first coordination shell, involving neighboring polyhedra, do not show clear signs of phase separation, which is expected as the phase separation spans over larger length scales. The investigation of the chemical arrangement of the glass building blocks at larger coordination shells is necessary. In Fig. 2, the evolution of the WC parameters in the second and third coordination shells of all considered compositions is represented. Comparing the results obtained from Fig. S6, which focuses on the first shell exclusively, with those presented in Fig. 2, a significant change in the WC parameter is observed for the Si–Si pair. α_{SiSi} calculated from, the second shell is positive at the composition with 90 mol% of SiO_2 and becomes negative with increasing Al_2O_3 content. This indicates that the second and third shells of Si prefer to have Si than Al, which is the first indication of the phase separation. The α_{AlAl} in the second and third shells remains negative and follows the same behavior as discussed earlier for the first shell. This finding indicates the preferred ordering between the AlO_n polyhedra. More interestingly,

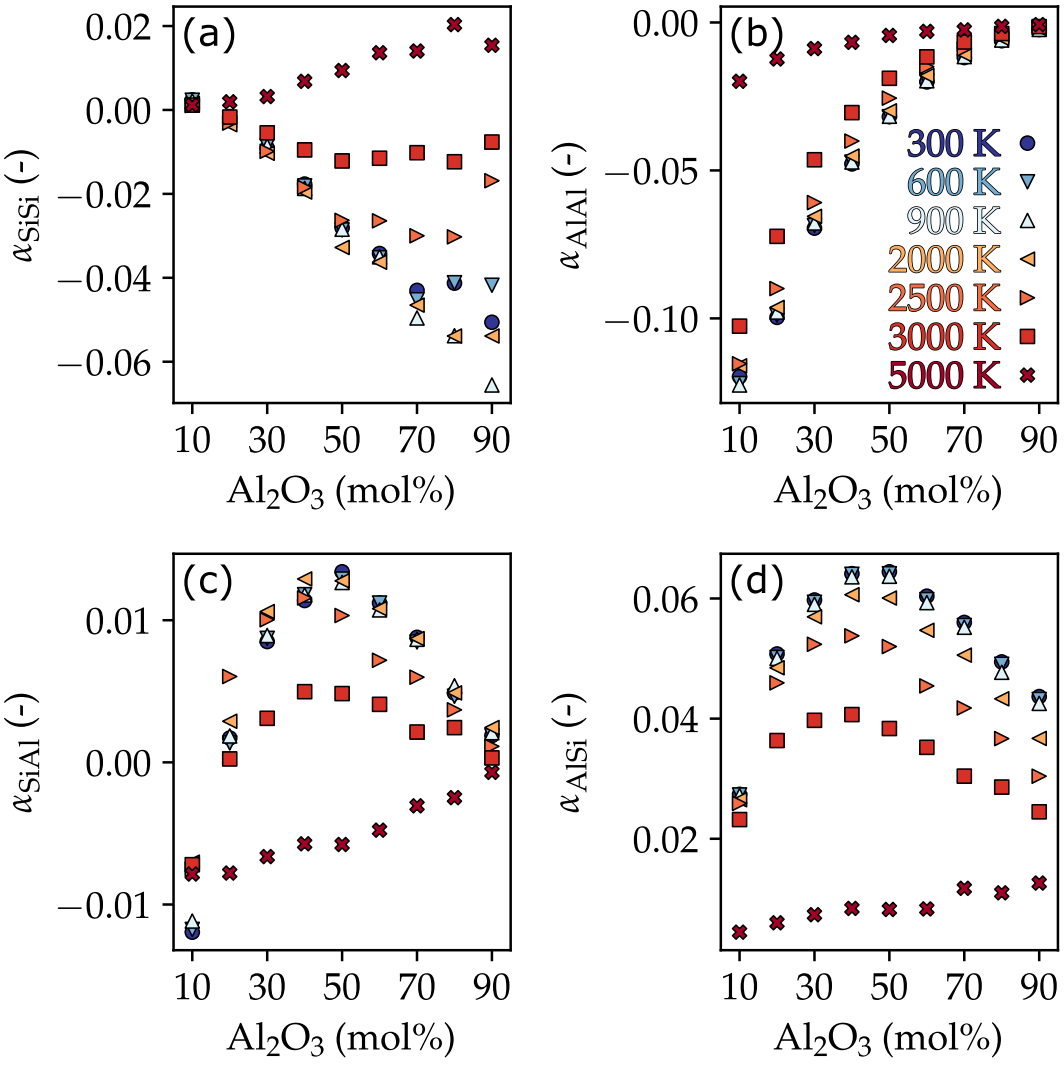

Fig. 3. Change of α_{ij} at the second shell as a function of the composition for different selected temperatures above and below T_g. (a) is for α_{SiSi}, (b) is for α_{All}, (c) is for α_{SiAl}, and (d) is for α_{AlSi}. The data for all samples as a function of the temperature is shown in Fig. S7. The standard error bars are smaller than the symbol size. The $r_{cut}^{2^{nd}shell} = 5.35$ Å. The values of the cutoff radii are provided for better reproducibility of the results. (For interpretation of the colors in the figure(s), the reader is referred to the web version of this article).

the WC parameter for the pairs Si–Al and Al–Si shows a maximum around $x = 0.5$, consistent with the data provided in Fig. 1(d). A gradual increase is observed for both pairs up to a maximum and decreases again. This shows that a maximum in the repulsion between SiO_4 tetrahedra and AlO_n polyhedra is around the composition at which R = $SiO_2/Al_2O_2 = 1$.

The temperature-dependent evolution of the WC parameter α_{SiSi}, α_{AlAl}, α_{SiAl}, and α_{AlSi} for the second shell is shown in Fig. 3 and used to investigate at which temperature the phase separation is manifested in the samples across all compositions. At elevated temperatures, the behavior of α_{SiSi} and α_{AlAl} of the second neighboring shell is similar to that at 300 K, with only the intensity being different. On the other hand, and at high temperatures, it is evident from the graph that the WC parameter of the α_{SiAl}, and α_{AlSi} tends towards lower values, negative in case of α_{SiAl}, and positive ones in case of α_{AlSi}, which indicate that in the liquid phase, SiO_4 attract AlO_n. The WC parameter becomes increasingly repulsive as the temperature decreases, particularly around the glass transition temperature (See Tab. S1 and Fig. S8). This suggests that aluminum polyhedra prefer to be surrounded by other aluminum polyhedra. This tendency promotes immiscibility in the supercooled liquid phase, leading to phase separation. The WC parameter shows that the sample exhibits a strong tendency towards demixing in the low-temperature region, as indicated by the higher positive values.

The findings presented in this study shed light on the origins of the nanoscale phase separation in binary aluminosilicate glasses. The repulsion between SiO_4 and AlO_n polyhedra is shown to be the origin of the phase separation in aluminosilicate glasses at the atomic scale. This phase separation was observed in previous experimental studies [26–28,31,33] and the MD work of Urata et al. [34]. Our analysis showed that the composition at which the phase separation is maximized in binary AS glasses is around 50 mol% of Al_2O_3.

The underlying hypothesis of this discussion is that phase separation refers to the redistribution of atoms from a homogeneous mixture to form distinct regions with different local atomic arrangements. This process occurs to minimize the energy of the system and to accommodate the differences in the local potential energy between different regions of the system. We computed the atomic potential energy for Si and Al to verify this hypothesis. The atomic potential energies ($\langle U_i \rangle$) were calculated for both Al and Si atoms. Subsequently, the variance of the potential energy per atom for each type of atom was calculated using the formula: $\sigma_i^2 = (1/N_i)(U_i\text{-}\langle U_i \rangle)^2$, where N_i represents the number of atoms of type i and U_i is the potential energy of atoms of type i. In Fig. 4(a), the variance obtained from the atomic potential energy distribution for both Si and Al atoms is shown. This shows that as the concentration of Al_2O_3 increases, there is a corresponding non-linear decrease in the variance for Al with a change of slope around 50

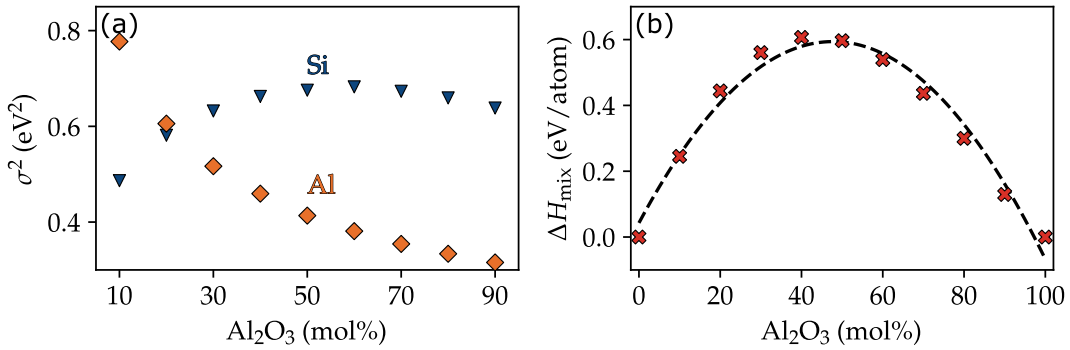

Fig. 4. (a) The variance of atomic potential energy for Si and Al atoms. (b) Variation of the mixing enthalpy as a function of alumina content at 300 K. The lines in (b) are to guide the eye (For interpretation of the colors in the figure(s), the reader is referred to the web version of this article).

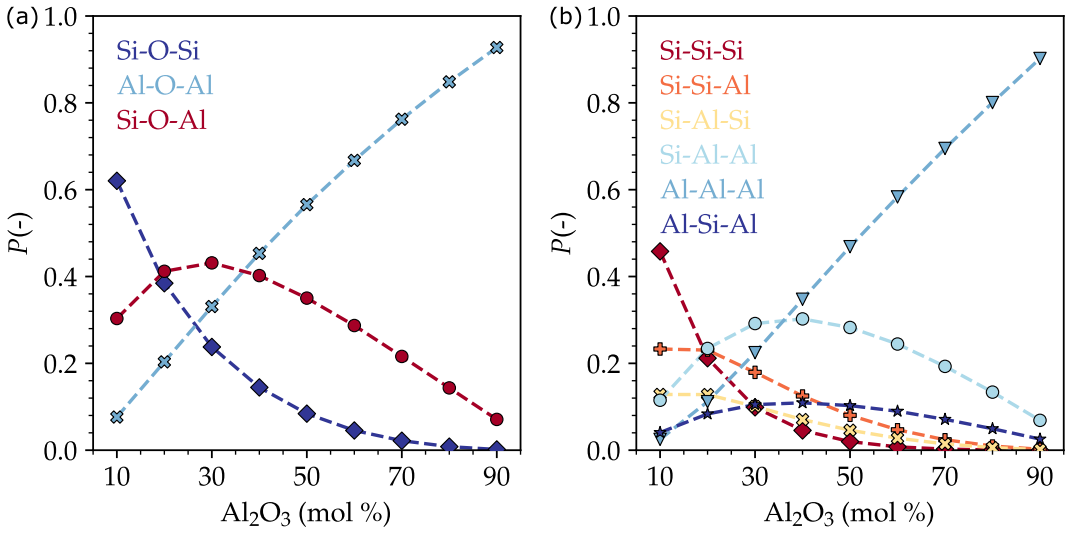

Fig. 5. (a) T–O–T and (b) T–T–T linkages (T is Si or Al) as a function of the Al_2O_3 content in the MD simulated AS glasses at 300 K.

mol% of Al_2O_3, indicating the local environment of Al becomes more homogeneous with increasing Al_2O_3 content.

On the other hand, this observation holds physical significance: the environment of SiO_4 tetrahedra is more homogeneous at low alumina content. With increasing Al_2O_3, the values of the variance increase to reach a maximum of around 50 mol% of Al_2O_3 and then decrease again. This also indicates that the highest deviation from the mean potential energy of Si atoms occurs when the Al_2O_3 content is approximately 50 mol%. This might be associated with the emergence of zones characterized by elevated potential energy. Such regions could signify areas where atomic interactions are less favorable, forming distinct phases. Thus, the phase separation in aluminosilicate glasses is due to a non-random distribution of the SiO_4 and AlO_n polyhedra, caused by the increasing attraction between SiO_4 tetrahedra and repulsion between SiO_4 tetrahedra and AlO_n polyhedra. These interactions between the network and the former polyhedra lead to the formation of distinct phases to minimize the system energy. This behavior is well captured by the positive mixing enthalpy ΔH_{mix} (detail of the calculation of ΔH_{mix} is given in the SM) obtained from the MD simulations, as shown in Fig. 4(b). For all compositions, the mixing enthalpy is positive, indicating the presence of a demixing in the glass, with its maximum being around 50 mol% of Al_2O_3. This is also in agreement with the observations made by Jantzen et al. [49], who suggested that the modulations below T_g are caused by structural density changes.

It is also known in the literature that the aluminum avoidance principle was proven to be violated in many aluminosilicate glasses, specifically when there is not enough Si in the glass to satisfy the aluminum avoidance principle [43,50]; however, if not enough Si atoms are available to satisfy the principle Al–O–Al bonds will form. These cases are well shown in Fig. 5(a), where we show the change of T–O–T with T is Si or Al as a function of Al_2O_3 content. The percentage of Al–O–Al linkage increases, while that of Si–O–Si decreases with increasing Al_2O_3 content. Moreover, in Fig. 5(b), the percentage of T–T–T linkages where T is Si or Al is depicted. The statistical analysis of T–T–T linkages demonstrates that with the increase of Al_2O_3, the Si–Si–Si, Si–Al–Si, and Si–Si–Al linkages decrease as a function of Al_2O_3 and the Al–Al–Al linkages increase linearly with alumina content. On the other hand, Si–Al–Al and Al–Si–Al increase to reach a maximum at around 40 mol% and decrease again. This supports the results observed from the WC parameter, where initially the glass is made of a Si-rich phase dominated by SiO_4 linkages, and as the Al_2O_3 content increases, an Al-rich and a mixed Si and Al phase coexist, which means the occurrence of phase separation. With further increase of Al_2O_3, the AlO_n phase dominates, which leads to the formation of a single phase again. It is to be stressed that the phase separation in mainly driven by a competition between entropy and enthalpy that force atoms to have the arrangement depicted above. This competition in the simulated glasses depends on the interatomic potential and the cooling rate used, which might led to a shift of the maximum phase separation to high Al_2O_3 content.

In summary, the current study has contributed to a clearer understanding of the origins of nanoscale phase separation in aluminosilicate glasses. We showed that compositions containing approximately 50 mol% of alumina exhibited the most pronounced phase separation. The origins of the nanoscale phase separation are caused by a preference for

SiO_4 and AlO_n polyhedra to cluster starting from the second neighboring shells, ultimately leading to the formation of distinct, homogeneous phases locally. This was demonstrated through the chemical order analysis at larger coordination shells using the WC parameter. Moreover, we showed that the phase separation is particularly pronounced in the vicinity of the glass transition temperature and continues to be notable at lower temperatures.

CRediT authorship contribution statement

Houssam Kharouji: Writing – original draft, Methodology, Investigation, Formal analysis. **Abdellatif Hasnaoui:** Writing – review & editing, Supervision. **Achraf Atila:** Writing – review & editing, Writing – original draft, Visualization, Methodology, Investigation, Formal analysis, Validation, Data curation, Conceptualization, Supervision.

Declaration of competing interest

The authors declare that they have no known competing financial interests or personal relationships that could have appeared to influence the work reported in this paper.

Acknowledgement

A.A gratefully acknowledges the computing resources provided by the Erlangen Regional Computing Center (RRZE) to run some simulations.

Appendix A. Supplementary data

Supplementary material related to this article can be found online at https://doi.org/10.1016/j.mtla.2024.102148.

References

[1] L. Wondraczek, E. Bouchbinder, A. Ehrlicher, J.C. Mauro, R. Sajzew, M.M. Smedskjaer, Advancing the mechanical performance of glasses: Perspectives and challenges, Adv. Mater. 34 (14) (2022) http://dx.doi.org/10.1002/adma.202109029.

[2] A. Atila, Y. Ouldhnini, S. Ouaskit, A. Hasnaoui, Atomistic insights into the mixed-alkali effect in phosphosilicate glasses, Phys. Rev. B 105 (13) (2022) 134101, http://dx.doi.org/10.1103/PhysRevB.105.134101.

[3] Y. Ouldhnini, A. Atila, S. Ouaskit, A. Hasnaoui, Atomistic insights into the structure and elasticity of densified 45s5 bioactive glasses, Phys. Chem. Chem. Phys. 23 (28) (2021) 15292–15301, http://dx.doi.org/10.1039/D1CP02192C.

[4] E. Axinte, Glasses as engineering materials: A review, Mater. Des. 32 (4) (2011) 1717–1732, http://dx.doi.org/10.1016/j.matdes.2010.11.057.

[5] J. Luo, J. Wang, E. Bitzek, J.Y. Huang, H. Zheng, L. Tong, Q. Yang, J. Li, S.X. Mao, Size-dependent brittle-to-ductile transition in silica glass nanofibers, Nano Lett. 16 (1) (2015) 105–113, http://dx.doi.org/10.1021/acs.nanolett.5b03070.

[6] A. Herrmann, A. Assadi, R. Lachheb, M. Zekri, A. Erlebach, K. Damak, R. Maalej, M. Sierka, C. Rüssel, The effect of glass structure and local rare earth site symmetry on the optical properties of rare earth doped alkaline earth aluminosilicate glasses, Acta Mater. 249 (2023) 118811, http://dx.doi.org/10.1016/j.actamat.2023.118811.

[7] G. Jagannath, A. Gaddam, S.V. Rao, D. Agarkov, G. Korableva, M. Ghosh, K.K. Dey, J.M. Ferreira, A.R. Allu, Tunable femtosecond nonlinear absorption and optical limiting thresholds of La_2O_3–B_2O_3 glasses by controlling the borate structural units, Scr. Mater. 211 (2022) 114530, http://dx.doi.org/10.1016/j.scriptamat.2022.114530.

[8] Y. Xiang, J. Du, M.M. Smedskjaer, J.C. Mauro, Structure and properties of sodium aluminosilicate glasses from molecular dynamics simulations, J. Chem. Phys. 139 (4) (2013) http://dx.doi.org/10.1063/1.4816378.

[9] A. Atila, E.M. Ghardi, S. Ouaskit, A. Hasnaoui, Atomistic insights into the impact of charge balancing cations on the structure and properties of aluminosilicate glasses, Phys. Rev. B 100 (14) (2019) 144109, http://dx.doi.org/10.1103/PhysRevB.100.144109.

[10] S. Ganisetti, A. Atila, J. Guénolé, A. Prakash, J. Horbach, L. Wondraczek, E. Bitzek, The origin of deformation induced topological anisotropy in silica glass, Acta Mater. 257 (2023) 119108, http://dx.doi.org/10.1016/j.actamat.2023.119108.

[11] Y. Bakhouch, S. Buchner, R.A. Silveira, L. Resende, A.S. Pereira, A. Hasnaoui, A. Atila, Pressure-driven homogenization of lithium disilicate glasses, J. Am. Ceram. Soc. (2024) http://dx.doi.org/10.1111/jace.19778.

[12] M.M. Smedskjaer, M. Bauchy, J.C. Mauro, S.J. Rzoska, M. Bockowski, Unique effects of thermal and pressure histories on glass hardness: Structural and topological origin, J. Chem. Phys. 143 (16) (2015) http://dx.doi.org/10.1063/1.4934540.

[13] T. Rouxel, S. Yoshida, The fracture toughness of inorganic glasses, J. Am. Ceram. Soc. 100 (10) (2017) 4374–4396, http://dx.doi.org/10.1111/jace.15108.

[14] A. Atila, E. Bitzek, Atomistic origins of deformation-induced structural anisotropy in metaphosphate glasses and its influence on mechanical properties, J. Non-Cryst. Solids 627 (2024) 122822, http://dx.doi.org/10.1016/j.jnoncrysol.2024.122822.

[15] Z. Pan, A. Atila, E. Bitzek, L. Wondraczek, Topology of anisotropic glasses from persistent homology analysis, J. Non-Cryst. Solids 627 (2024) 122801, http://dx.doi.org/10.1016/j.jnoncrysol.2023.122801.

[16] Y. Zhang, L. Huang, Y. Shi, Towards damage resistant Al_2O_3–SiO_2 glasses with structural and chemical heterogeneities through consolidation of glassy nanoparticles, Acta Mater. 215 (2021) 117016, http://dx.doi.org/10.1016/j.actamat.2021.117016.

[17] K. Januchta, R.E. Youngman, A. Goel, M. Bauchy, S.J. Rzoska, M. Bockowski, M.M. Smedskjaer, Structural origin of high crack resistance in sodium aluminoborate glasses, J. Non-Cryst. Solids 460 (2017) 54–65, http://dx.doi.org/10.1016/j.jnoncrysol.2017.01.019.

[18] K. Januchta, R.E. Youngman, A. Goel, M. Bauchy, S.L. Logunov, S.J. Rzoska, M. Bockowski, L.R. Jensen, M.M. Smedskjaer, Discovery of ultra-crack-resistant oxide glasses with adaptive networks, Chem. Mater. 29 (14) (2017) 5865–5876, http://dx.doi.org/10.1021/acs.chemmater.7b00921.

[19] G.A. Rosales-Sosa, A. Masuno, Y. Higo, H. Inoue, Crack-resistant al2o3-sio2 glasses, Sci. Rep. 6 (2016) 23620, http://dx.doi.org/10.1038/srep2362.

[20] Y. Shi, J. Luo, F. Yuan, L. Huang, Intrinsic ductility of glassy solids, J. Appl. Phys. 115 (4) (2014) http://dx.doi.org/10.1063/1.4862959.

[21] Z. Yin, F. Hannard, F. Barthelat, Impact-resistant nacre-like transparent materials, Science 364 (6447) (2019) 1260–1263, http://dx.doi.org/10.1126/science.aaw8988.

[22] F. Yuan, L. Huang, Brittle to ductile transition in densified silica glass, Sci. Rep. 4 (1) (2014) http://dx.doi.org/10.1038/srep05035.

[23] L. Tang, N.M.A. Krishnan, J. Berjikian, J. Rivera, M.M. Smedskjaer, J.C. Mauro, W. Zhou, M. Bauchy, Effect of nanoscale phase separation on the fracture behavior of glasses: Toward tough yet transparent glasses, Phys. Rev. Mater. 2 (11) (2018) http://dx.doi.org/10.1103/physrevmaterials.2.113602.

[24] B. Wang, Y. Yu, M. Wang, J.C. Mauro, M. Bauchy, Nanoductility in silicate glasses is driven by topological heterogeneity, Phys. Rev. B 93 (6) (2016) http://dx.doi.org/10.1103/physrevb.93.064202.

[25] F. Xia, X. Wang, Y. Wang, X. Ren, A. Qiao, H. Tao, Tuning the hardness and crack resistance through liquid–liquid phase separation in an aluminosilicate glass, Phys. Chem. Chem. Phys. 25 (26) (2023) 17619–17626, http://dx.doi.org/10.1039/d3cp02506c.

[26] J.F. Macdowell, G.H. Beall, Immiscibility and crystallization in Al_2O_3-SiO_2 glasses, J. Am. Ceram. Soc. 52 (1) (1969) 17–25, http://dx.doi.org/10.1111/j.1151-2916.1969.tb12653.x.

[27] S.H. Risbud, J.A. Pask, Calculated thermodynamic data and metastable immiscibility in the system SiO_2-Al_2O_3, J. Am. Ceram. Soc. 60 (1977) 418, http://dx.doi.org/10.1111/j.1151-2916.1977.tb15525.x.

[28] F.J. Klug, S. Prochazka, R.H. Doremus, Alumina-silica phase diagram in the mollite region, J. Am. Ceram. Soc. 70 (10) (1987) 750–759, http://dx.doi.org/10.1111/j.1151-2916.1987.tb04875.x.

[29] B.T. Poe, P.F. McMillan, C. Angell, R. Sato, Al and Si coordination in SiO_2-Al_2O_3 glasses and liquids: A study by NMR and IR spectroscopy and MD simulations, Chem. Geol. 96 (3–4) (1992) 333–349, http://dx.doi.org/10.1016/0009-2541(92)90063-b.

[30] M. Djuric, A. Mihajlov, L. Petrasinovic-Stojkanovic, B. Zivanovic, Thermodynamic analysis of the metastable regions for the Al_2O_3-SiO_2 system, J. Am. Ceram. Soc. 79 (5) (1996) 1252–1256, http://dx.doi.org/10.1111/j.1151-2916.1996.tb08580.x.

[31] S.K. Wilke, C.J. Benmore, J. Ilavsky, R.E. Youngman, A. Rezikyan, M.P. Carson, V. Menon, R. Weber, Phase separation in mullite-composition glass, Sci. Rep. 12 (1) (2022) http://dx.doi.org/10.1038/s41598-022-22557-7.

[32] T. Ohkubo, A. Masuno, E. Tsuchida, S. Ohki, Theoretical insights into the ^{27}Al NMR parameters of binary aluminosilicate glass and their relationship to the atomic and electronic structure, J. Phys. Chem. C 128 (3) (2024) 1298–1311, http://dx.doi.org/10.1021/acs.jpcc.3c06292.

[33] S.K. Wilke, C.J. Benmore, V. Menon, J. Ilavsky, A. Rezikyan, R.E. Youngman, M.P. Carson, R. Weber, Revisiting metastable immiscibility in SiO_2–Al_2O_3: Structure and phase separation of supercooled liquids and glasses, J. Am. Ceram. Soc. 106 (5) (2023) 2820–2834, http://dx.doi.org/10.1111/jace.18960.

[34] S. Urata, N. Nakamura, T. Tada, H. Hosono, Molecular dynamics study on the co-doping effect of al2o3 and fluorine to reduce rayleigh scattering of silica glass, J. Am. Ceram. Soc. 104 (10) (2021) 5001–5015, http://dx.doi.org/10.1111/jace.17774.

[35] P. Hudon, D.R. Baker, The nature of phase separation in binary oxide melts and glasses.i.silicate systems, J. Non-Cryst. Solids 303 (3) (2002) 299–345, http://dx.doi.org/10.1016/s0022-3093(02)01043-8.

[36] S. Sen, R.E. Youngman, High-resolution multinuclear NMR structural study of binary aluminosilicate and other related glasses, J. Phys. Chem. B 108 (23) (2004) 7557–7564, http://dx.doi.org/10.1021/jp031348u.

[37] K. Liao, A. Masuno, A. Taguchi, H. Moriwake, H. Inoue, T. Mizoguchi, Revealing spatial distribution of al-coordinated species in a phase-separated aluminosilicate glass by STEM-EELS, J. Phys. Chem. Lett. 11 (22) (2020) 9637–9642, http://dx.doi.org/10.1021/acs.jpclett.0c02687.

[38] L. Martel, M. Allix, F. Millot, V. Sarou-Kanian, E. Véron, S. Ory, D. Massiot, M. Deschamps, Controlling the size of nanodomains in calcium aluminosilicate glasses, J. Phys. Chem. C 115 (39) (2011) 18935–18945, http://dx.doi.org/10.1021/jp200824m.

[39] H. Sreenivasan, P. Kinnunen, E. Adesanya, M. Patanen, A.M. Kantola, V.-V. Telkki, M. Huttula, W. Cao, J.L. Provis, M. Illikainen, Field strength of network-modifying cation dictates the structure of (na-mg) aluminosilicate glasses, Front. Mater. 7 (2020) http://dx.doi.org/10.3389/fmats.2020.00267.

[40] A.P. Thompson, H.M. Aktulga, R. Berger, D.S. Bolintineanu, W.M. Brown, P.S. Crozier, P.J. in't Veld, A. Kohlmeyer, S.G. Moore, T.D. Nguyen, R. Shan, M.J. Stevens, J. Tranchida, C. Trott, S.J. Plimpton, LAMMPS - a flexible simulation tool for particle-based materials modeling at the atomic meso, and continuum scales, Comput. Phys. Comm. 271 (2022) 108171, http://dx.doi.org/10.1016/j.cpc.2021.108171.

[41] M. Bouhadja, N. Jakse, Pasturel, structural and dynamic properties of calcium aluminosilicate melts: A molecular dynamics study, J. Chem. Phys. 138 (22) (2013) 224510, http://dx.doi.org/10.1063/1.4809523.

[42] M. Bouhadja, N. Jakse, Structural and dynamic properties of aluminosilicate melts: a molecular dynamics study, J. Phys.: Condens. Matter. 32 (10) (2019) 104002, http://dx.doi.org/10.1088/1361-648x/ab58ea.

[43] A. Atila, E.M. Ghardi, A. Hasnaoui, S. Ouaskit, Alumina effect on the structure and properties of calcium aluminosilicate in the percalcic region: A molecular dynamics investigation, J. Non-Cryst. Solids 525 (2019) 119470, http://dx.doi.org/10.1016/j.jnoncrysol.2019.119470.

[44] A. Stukowski, Visualization and analysis of atomistic simulation data with ovito–the open visualization tool, Modelling Simul. Mater. Sci. Eng. 18 (1) (2009) 015012, http://dx.doi.org/10.1088/0965-0393/18/1/015012.

[45] M. Bauchy, Structural, vibrational, and elastic properties of a calcium aluminosilicate glass from molecular dynamics simulations: The role of the potential, J. Chem. Phys. 141 (2) (2014) http://dx.doi.org/10.1063/1.4886421.

[46] R. Weber, S. Sen, R.E. Youngman, R.T. Hart, C.J. Benmore, Structure of high alumina content Al_2O_3-SiO_2 composition glasses, J. Phys. Chem. B 112 (2008) 16726, http://dx.doi.org/10.1021/jp807964u.

[47] T. Ban, S. Hayashi, A. Yasumori, K. Okada, Calculation of metastable immiscibility region in the Al_2O_3-SiO_2 system, J. Mater. Res. 11 (6) (1996) 1421–1427, http://dx.doi.org/10.1557/jmr.1996.0178.

[48] J.M. Cowley, An approximate theory of order in alloys, Phys. Rev. 77 (5) (1950) 669–675, http://dx.doi.org/10.1103/physrev.77.669.

[49] C. Jantzen, D. Schwahn, J. Schelten, H. Herman, Phase decomposition in Al_2O_3–SiO_2 glasses, J. Appl. Crystallogr. 11 (5) (1978) 614–615, http://dx.doi.org/10.1107/s0021889878014028.

[50] A.R. Allu, A. Gaddam, S. Ganisetti, S. Balaji, R. Siegel, G.C. Mather, M. Fabian, M.J. Pascual, N. Ditaranto, W. Milius, J. Senker, D.A. Agarkov, V.V. Kharton, J.M.F. Ferreira, Structure and crystallization of alkaline-earth aluminosilicate glasses: Prevention of the alumina-avoidance principle, J. Phys. Chem. B 122 (17) (2018) 4737–4747, http://dx.doi.org/10.1021/acs.jpcb.8b01811.